

EXPERIMENTAL AND NUMERICAL STUDIES ON VIBRATION PROPAGATION

Arja Saarenheimo¹, Kim Calonius², Alexis Fedoroff³, Markku Tuomala⁴ and Ari Vepsä⁵

¹ Research Team Leader, VTT Technical Research Centre of Finland Ltd

² Senior Scientist, VTT Technical Research Centre of Finland Ltd

³ Research Scientist, VTT Technical Research Centre of Finland Ltd

⁴ Prof. emeritus, Consultant, Finland

⁵ Senior Scientist, VTT Technical Research Centre of Finland Ltd

ABSTRACT

A test series called V1 considering vibration propagation has been carried out at VTT. The test target is a reinforced concrete structure with two vertical parallel walls connected to a floor slab. The front wall is additionally supported by triangular shaped side walls which are also connected to the floor slab. The test structure is vertically supported on elastomeric bearing pads and tension bars and horizontally supported with steel back pipes effective mainly in compression and with steel bars effective in tension. In order to obtain information on vibration propagation in damaged concrete structure at different levels of damage grades the same structure was tested six times. At each time the mass of the deformable stainless steel missile was 50 kg. The hit point was located in the middle of the front wall. The impact velocity was about 110 m/s in the first four tests (V1A-D) and about 60 m/s in the remaining two tests (V1E and F).

In this paper, the experimental setup is described and calculated results on Test V1A, such as accelerations, displacements, their response spectra and strains are compared with corresponding experimental measurements. Concrete damage plasticity model is adopted in Abaqus models. Additionally an in-house (IHC) code was used for comparison calculations. This code uses relations between stress resultants and generalised strains or alternatively a layered approach is used. Sensitivity studies on the effect of concrete material parameters to vibration behaviour are carried out.

INTRODUCTION

The primary task of protective walls is to keep possible impacting projectiles and burning fuel outside the building housing vulnerable equipment protecting them against external loads. The design of safety related structures considering vibration isolation, e.g. nuclear power plants, requires reliable analysis methods that are verified against relevant test results. Operability of sensitive equipment vital for plant safety may be lost due to heavy vibrations resulting from impact load.

Vibration propagation test series V, which is a part of an experimental programme conducted at VTT concerning impact loaded concrete structures, was initiated with a test called V0 (Vepsä et al., 2015). Test structure V0 was supported with a steel frame in a similar way as the slab specific tests earlier in related test series. Based on experience with V0 the next test structure V1 was designed so that the use of supporting frame could be avoided. In this way, damping effect would remain as much as practically possible in the V1 structure itself. The specimen rests on elastomeric bearing pads and it is additionally supported in horizontal and vertical directions.

Test series V was designed for studying the propagation of vibrations in concrete structures. The front wall is gradually damaged due to consecutive impacts. The floor and rear wall experience less nonlinear

behaviour. This simulates the circumstances in rooms enveloped by massive reinforced concrete walls and floors, where protected SSCs receive external vibrations from damaged structures.

Damping is an important factor influencing the response of structures during impact and especially when studying the propagation of vibrations in concrete structures. Sensitivity studies on damping are presented in Saarenheimo (2017).

TEST

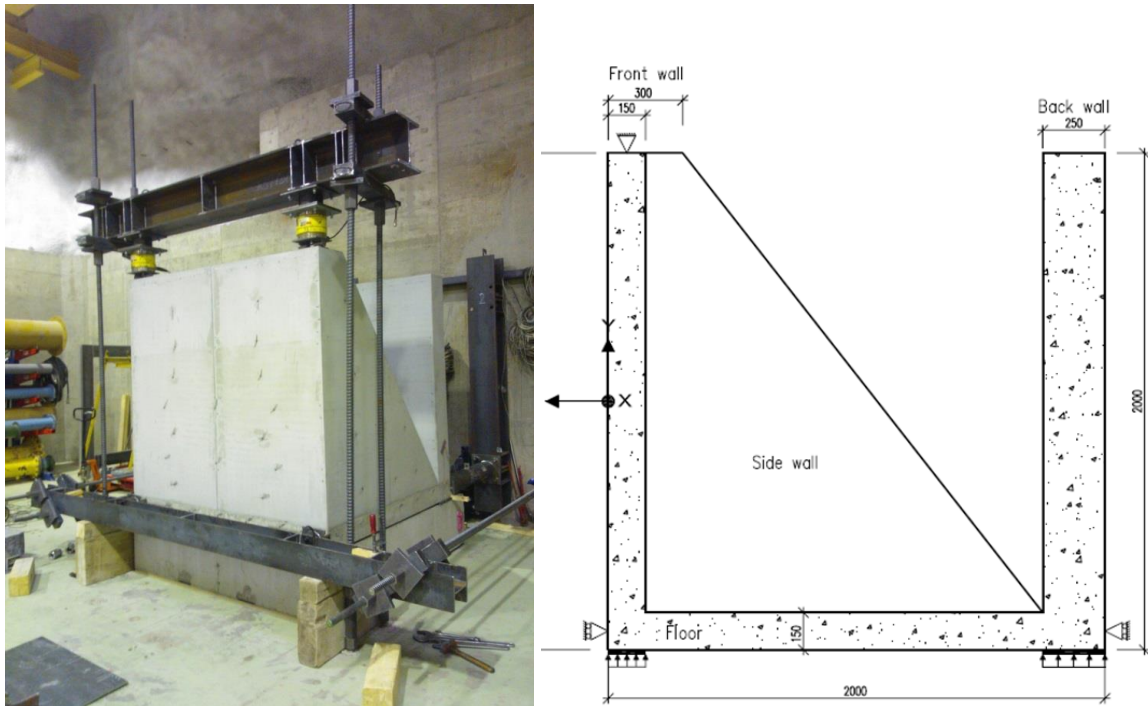


Figure 1. Reinforced concrete target with side view on the right hand side.

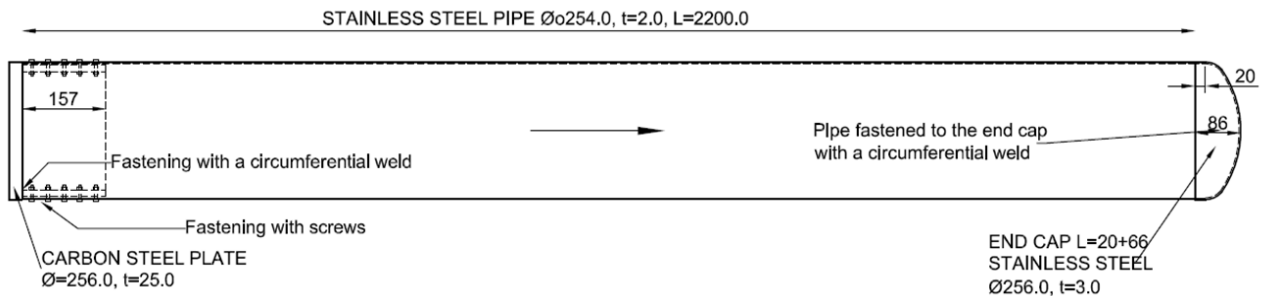


Figure 2. Stainless steel missile with a mass of 50 kg. Dimensions are in [mm].

The main purpose of test V1 is to study propagation and damping of vibration caused by impacts of deformable missiles. Reinforced concrete test structure is presented in Figure 1 with some main dimensions in [mm]. The thickness of the front wall, triangular shaped side walls and floor slab is 0.15 m and the thickness of the rear wall is 0.25 m. The width of the structure is 2.0 m and the span width of the front wall is 1.85 m. There are 20 mm thick elastomeric bearings below the front wall and the rear wall. The vertical support system of the front wall is anchored to the basement with Dywidag bars of 40 mm diameter and with an effective length of about 2.9 m. Short back pipes, with a length of about 1.1 m, at

the lower edge of the rear wall are connected to the base rock in order to prevent the horizontal displacement to the loading direction. Horizontally located Dywidag bars with a diameter of 32 mm and length of 3.7 m are utilised to prevent the movement of the target against the loading direction. These Dywidag bars are anchored to the base rock.

The cylindrical compressive strength of concrete has been tested as 53.7 MPa for the floor slab and 47.2 MPa for the walls. The main longitudinal (bending) reinforcement was made with 6 mm diameter rebars with a spacing of 50 mm and yield strength of 626 MPa. Stirrups of 6 mm diameter were arranged at a spacing of 100 mm in the impact area of the front wall.

The missile is shown in Figure 2. The main part is a stainless steel pipe with a wall thickness of 2 mm. The wall thickness of the cap in the front of the missile is 3 mm. A steel plate is added to the rear end of the missile in order to increase the total mass to 50 kg. The hit point is in the middle of the front wall and the impact velocity in the considered test V1A is 113.6 m/s. This type of missile has been used in many tests before and also with the same impact velocity.

FINITE ELEMENT MODELS

Abaqus model

Nonlinear structural analyses were carried out with Abaqus/Explicit code, Abaqus (2014). Finite element (FE) mesh of the reinforced concrete mock-up model is presented in Figure 3 on the left side. Four noded shell elements with the Gaussian one point reduced integration rule are used. The number of elements is 5800. The average length of the element edge is 5 cm and there are fifteen Simpson integration points through the shell thickness. Nonlinear behaviour of concrete is modeled with the concrete damaged plasticity model. Reinforcement is modeled as layers using an elastic plastic material model with isotropic yield hardening and the von Mises yield condition. Shear reinforcement is not considered. The impact load is introduced to the structure as a pressure transient the impact area of which is indicated by red colour in Figure 3 on the left side. The force-time function is presented in Figure 5a.

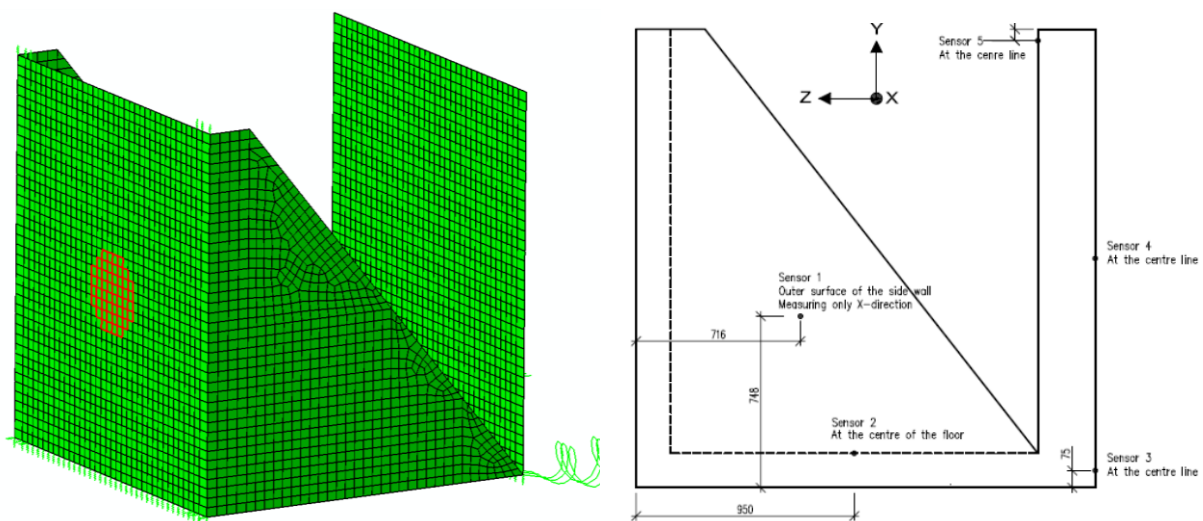


Figure 3. Shell element model and locations of accelerometers.

The effect of tensile cracking properties on vibration propagation was studied by varying the concrete property material parameters related to tensile behaviour. Tensile fracture energy was assumed to be 100 J/m² and 150 J/m². Also, the assumed stress-strain relationship of the cracked concrete was varied. Linear

and bilinear assumptions made for tensile cracking behaviour of concrete as a function of strain are shown in Figure 4. These fracture stress assumptions are based straightforwardly on the tensile splitting material test results and stress-strain dependency is adjusted according to the element size in order to avoid mesh dependency.

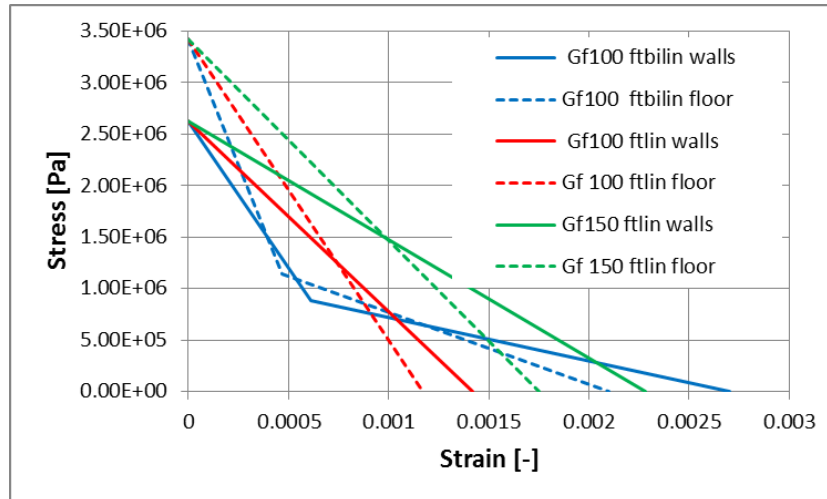


Figure 4. Tensile post-cracking properties for concrete (characteristic length 0.05 m).

IHC model

A 24-degree-of-freedom (24 DOF) flat shell element is used in the computations of the vibration test with and in-house code (IHC). The element is constructed by combining a plate element and a membrane element and using a coordinate transformation from local to global coordinate system. The degrees of freedom of the shell element in local frame are: u , v , w , θ_x , θ_y and θ_z (3 translations and 3 rotations). The rotation corresponding to the local rotation θ_z is restrained except at shell junctions where two elements meet at an angle different from π .

The plate part of the element is constructed according to the Reissner-Mindlin theory. Bilinear polynomial interpolation is used for the deflection and the rotations. In computing the transverse shear strains covariant transverse shear strain assumption and interpolation is adopted, Bathe and Dvorkin (1985). The von Karman definition of nonlinear Lagrangian strain is used in computing the membrane strains. Material nonlinearities are formulated in terms of stress resultants and curvatures in a similar fashion as e.g. in Ibrahimcovic and Frey (1993) and Koechlin and Potapov (2007). Interaction between the bending resultants is taken into account. In reverse motion, cracked state stiffness is assumed. Yield condition is defined in terms of strains and stress resultants. Separate yield condition is used for transverse shear forces. Results obtained with stress resultant approach are indicated by ‘IHC res’. Additionally also the layered model is used. In the layered version of the IHC a rectangular plane stress yield condition in terms of principal stresses is assumed in each concrete layer and unlike in Abaqus the so called rotating crack approach is adopted. For defining the concrete behaviour in cracked state the fracture energy concept is utilized similarly as in Abaqus with a linear stress strain curve in post crack state. Reinforcing steel bars are modelled with separate layers with individual positions in thickness direction for each layer as in Abaqus. There are nine layers for concrete and four layers for reinforcement. Calculation results obtained with the layered model are indicated by ‘IHC layer’.

The assumed Rayleigh damping ratio is 0.05 at frequencies 45 and 1000 Hz. Gravity load is imposed during the first analysis phase of 0.1 s. Pressure-time function is applied for the impact load in the consecutive analysis step simulating the tests V1A.

Boundary conditions

The support structures were modelled with nonlinear spring elements in both Abaqus and IHC models. The elastomeric pads under the walls are modelled with lines of spring elements beneath the walls corresponding to a stiffness $k = 100 \text{ MN/m}^3$ estimated from Calenberg Ingenieure GmbH (2016), effective only in compression. Dywidag bars and back pipes are also modelled with spring elements with spring stiffness properties determined based on the design drawings. Masses of supporting system are added to the computational models. For HEB300 $m = 117 \text{ kg/m}$. The mass of the supporting system above the front wall becomes about 400 kg.

Additionally, in the Abaqus model there are two vertical springs at the corners of the rear wall lower edge. Based on the preliminary studies and observations, the horizontal back pipes located at the corners of the lower edge act also as vertical supports. This is due to the fact that the structure is tightened with horizontally located Dywidag bars against the back pipes. Stiffness properties of these additional spring elements were tuned by adjusting the numerical vertical displacement with the corresponding measured value. Stiffness properties are summarised in Table 1.

Table 1: Spring stiffnesses.

Front wall lower edge horizontal (at both corners against loading direction)	Front wall lower edge vertical (downwards only)	Front wall upper edge vertical (at both corners upwards only)	Rear wall lower edge horizontal (at both corners in loading direction)	Rear wall lower edge vertical (at both corners) Abaqus model	Rear wall lower edge vertical (downwards only)
9.13 MN/m	32.25 MN/m	129 MN/m	1204 MN/m	downwards 48 MN/m upwards 12 MN/m	53.7 MN/m

Load

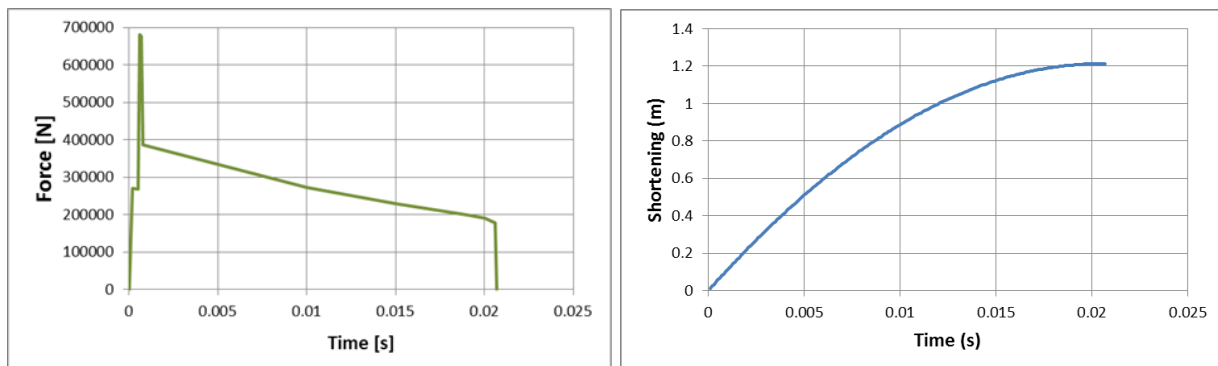


Figure 5. a) Force-time function and b) crushed length as a function of time.

The load function was calculated by the Riera method (Riera, 1968) by assuming a visco-plastic folding mechanism and adopting the material property values $E = 200 \text{ GPa}$, $\sigma_y = 400 \text{ MPa}$, $\rho = 7850 \text{ kg/m}^3$ and parameter values $D = 1522$ and $q = 5.13$ for the Cowper-Symonds 1-D visco-plastic model. The calculated force time function is depicted in Figure 5a and the shortening of the missile as a function of

time is shown in Figure 5b. The calculated duration of the impact is 21 ms and the corresponding one observed during the test was 19 ms. Shortening of the missile according to the Riera method is 1.2 m. The corresponding observed length after the test was also about 1.2 m.

RESULTS

Displacements

Comparison of calculation results obtained with three different models, Abaqus, IHC with the stress resultant approach (IHC res) and with the layered approach (IHC layer) are presented below on the left hand side (Figs a). Sensitivity studies on tensile fracture behaviour properties were carried out with the Abaqus model and these results are presented on the right hand side figures (Figs b). Calculated horizontal displacements in the middle of the impact location are shown with the corresponding measured result in Figure 6a and 6b. Calculation results obtained with IHC are presented in Figure 6a with the result calculated by Abaqus model assuming a similar post tensile behaviour with fracture energy 100 J/m^2 and a linear tensile stress decrease after tensile cracking. The maximum displacement is predicted most accurately by IHC applying the stress resultant method. The permanent deflections are somewhat underestimated by IHC. Sensitivity study results carried out with Abaqus code are shown in Figure 6b. Maximum displacements obtained with the lower tensile fracture energy assumption (100 J/m^2) are closer to the measured value than the corresponding results obtained by assuming a fracture energy value of 150 J/m^2 . Permanent displacements obtained by using linear post-tensile fracture stress-strain relationship are all in a quite good agreement with the corresponding measurements.

Calculated and measured horizontal displacements at the top of the rear wall are presented in Figures 7a and 7b. Bending vibration of the rear wall is most accurately predicted by IHC. Calculated and measured vertical displacements of the rear wall are presented in Figure 8a and 8b. Vertical displacement results obtained with IHC are presented in Figure 8a with the measurement result. Also the comparable displacement result obtained with the Abaqus model is shown. Without the additional adjusted vertical spring supports used in the Abaqus model, the calculated vertical displacements are larger than the corresponding measured ones. The effect of the adjusted vertical support in Abaqus model can clearly be seen here. In Figure 8b, the maximum displacements upwards and downwards are in agreement with the measurement result.

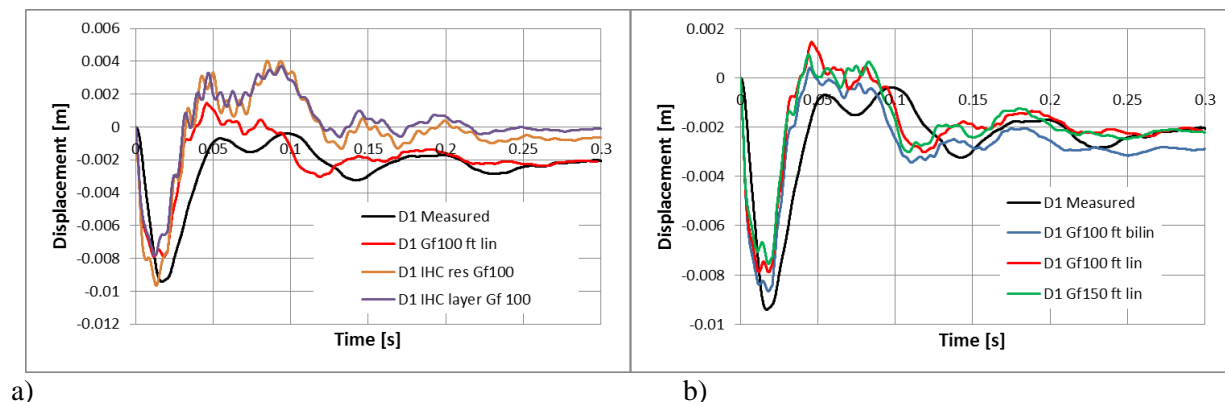
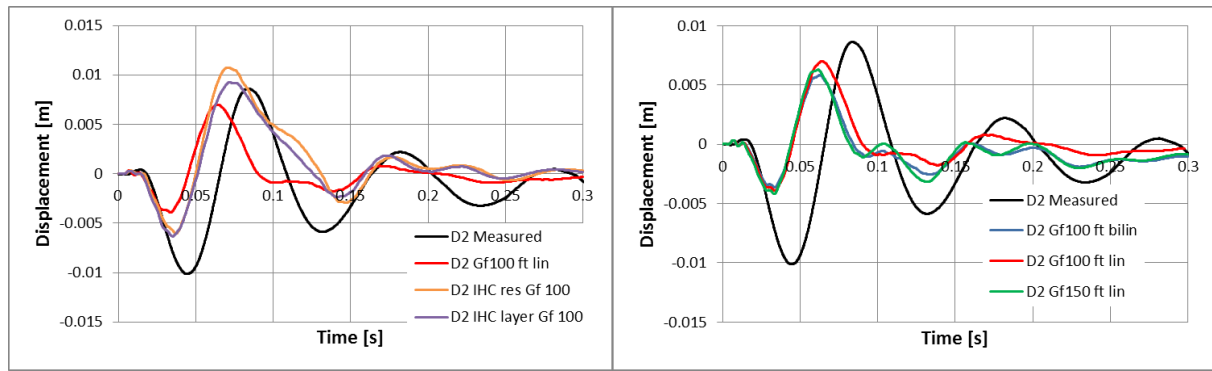
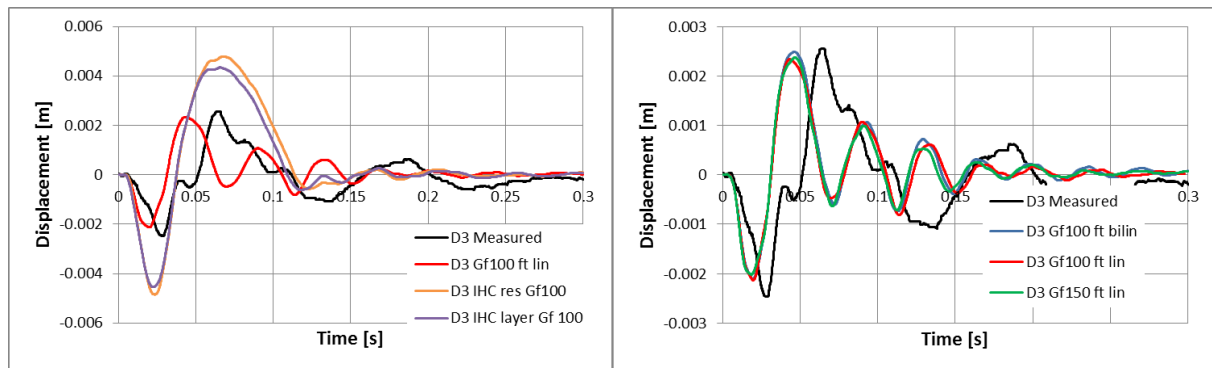


Figure 6. Horizontal displacement at the impact location, a) results obtained using different analysis codes, b) effect of tensile cracking assumption.

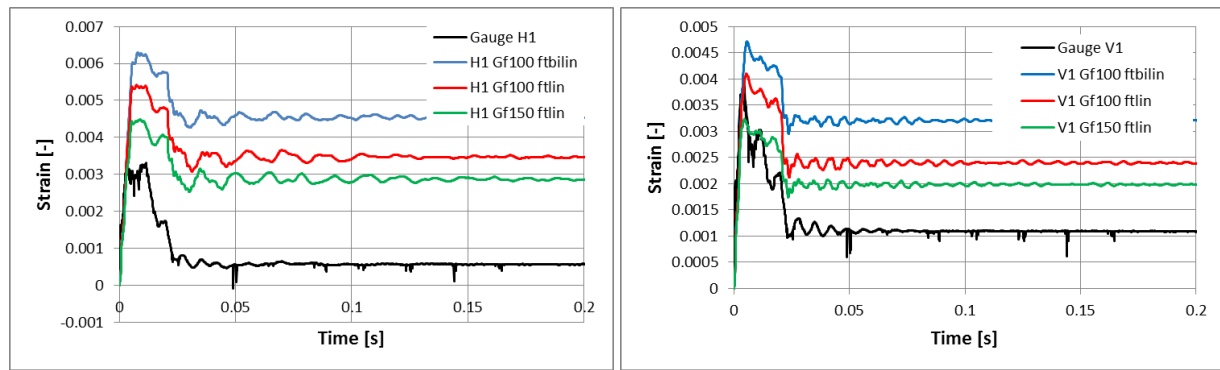


a) b)
 Figure 7. Horizontal displacement at the top of the back wall, a) results obtained using different analysis codes, b) effect of tensile cracking assumption.



a) b)
 Figure 8. Vertical displacement of the rear wall, a) results obtained using different analysis codes. b) effect of tensile cracking assumption.

Strains in reinforcement



a) b)
 Figure 9. Strain at the a) horizontal and b) vertical back surface reinforcement.

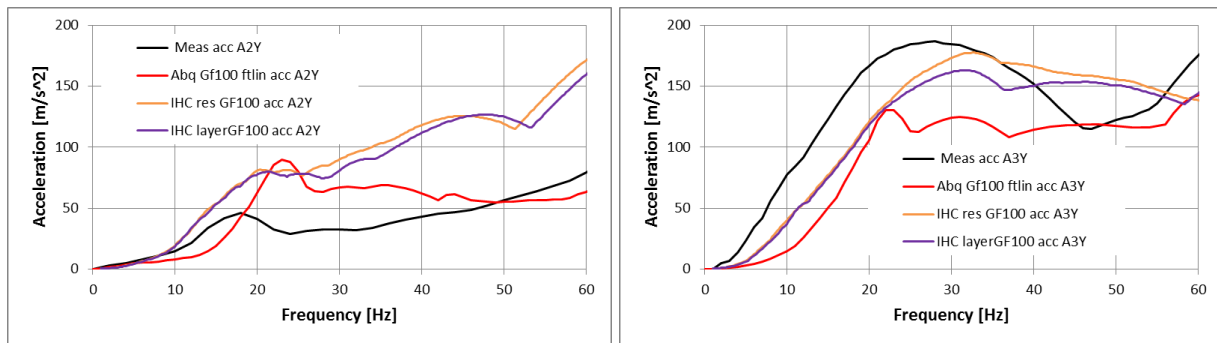
Calculated and measured strains in the horizontal (Gauge H1) and vertical (Gauge V1) back surface reinforcement in the middle of the impact area are presented in Figure 9a and 9b as functions of time. These strain results were obtained by the Abaqus model varying the tensile cracking assumption. Both the measured and the calculated strain values are rather low, staying below 1%. It should be noted that yielding in reinforcement is most probable very local and thus these values are not necessarily perfectly

comparable. The assumed tensile cracking behaviour clearly has an effect on yielding of the reinforcement.

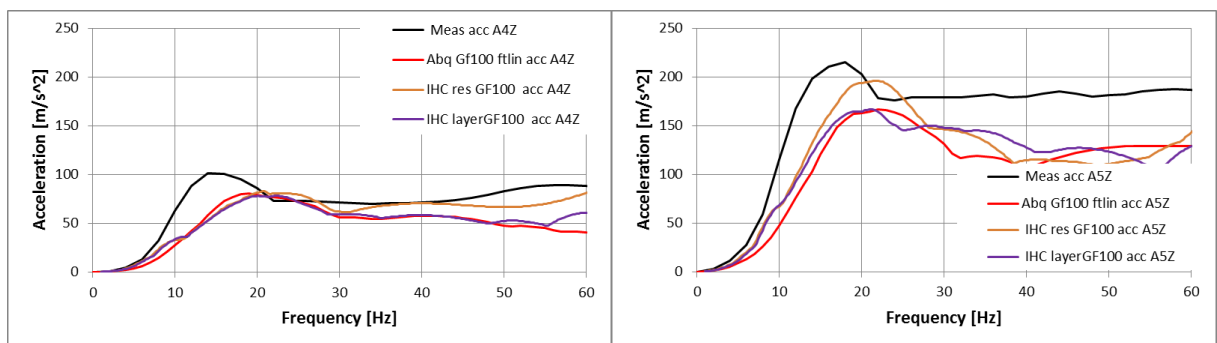
Response spectra

Floor response spectra are computed from the measured and calculated acceleration results adopting a 5% damping. For the measured acceleration spectra the filtered values less than 250 Hz are applied. Locations of the accelerometers (A1-A5) are shown in Figure 3 on the right.

Acceleration spectra values obtained with Abaqus model and with the IHC models assuming a linear tensile stress decrease after cracking are compared with the corresponding measurement results in Figure 10 and in Figure 11. Vertical acceleration spectra results obtained in the middle of the floor slab (Sensor 2) are presented in Figure 10a and the corresponding values at the floor to rear wall junction are shown in Figure 10b. In the middle of the floor, at frequencies below 10 Hz the acceleration spectra are accurately predicted with the both IHC models. At the frequencies over 10 Hz the IHC model overpredicts the result. Corresponding results at the floor rear wall junction (Sensor 3) are presented in Figure 10b. The Abaqus model clearly underestimates the acceleration response spectra. The both results obtained with the IHC model are in a better agreement with the measurement result. But they also underestimate the acceleration spectra at the frequencies below 30 Hz. The acceleration spectra obtained with the stress resultant approach is quite close to the corresponding measurement result.



a) b)
 Figure 10. Vertical acceleration spectra in the floor, a) middle of the floor and b) at the floor to rear wall junction, comparison of different analysis codes.



a) b)
 Figure 11. Horizontal acceleration spectra at the rear wall, a) middle of the wall height and b) at the top, comparison of different analysis codes.

Horizontal acceleration spectra results obtained in the middle height of the rear wall (Sensor 4) and at the top of the rear wall (Sensor 5) are presented in Figure 11a and 11b, respectively. Acceleration spectra

results obtained by different methods are quite similar and are also in a good agreement with the corresponding measurement results.

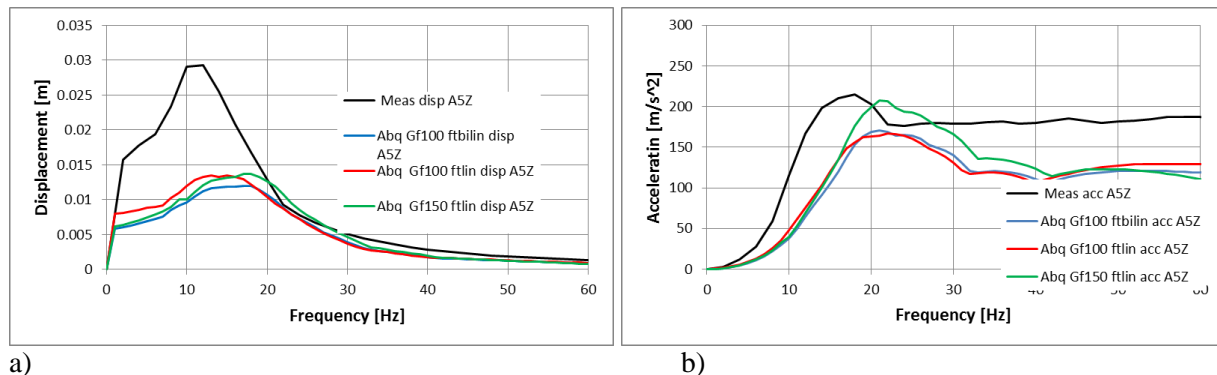


Figure 12. Displacement and acceleration spectra at the top of the rear wall in the horizontal direction showing the effect of tensile cracking assumption.

The effect of different types of tensile fracture behaviour was studied using the Abaqus model. The displacement spectra values shown in Figure 12a are less than 2 mm at the frequencies over 50 Hz and thus the acceleration spectra results at the higher frequency range are of minor importance and not considered here. Higher response spectra values are obtained with the higher tensile fracture energy assumption. The assumed post tensile fracture stress strain relationship does not affect considerably the acceleration spectra result. When the lower fracture energy assumption, 100 J/m², was applied the energy dissipated by tensile cracking and by yielding of the reinforcement becomes higher and thus the obtained acceleration spectra values are lower.

CONCLUSION

Maximum deflection at the hit point was most accurately predicted by IHC using the stress resultant approach. Based on the sensitivity studies carried out with the Abaqus model, the calculated maximum displacement value at the hit point is somewhat dependent on the assumed tensile cracking behaviour. In the considered cases, the assumed tensile fracture energy is not affecting the permanent displacement. Bilinear post-tensile stress decrease assumption leads to larger maximum and permanent deflection values than the ones obtained with the corresponding linear assumption.

Higher frequency response spectra values were obtained when the higher tensile fracture energy assumption was used. With the lower fracture energy assumption more energy will be dissipated due to permanent deformations such as concrete cracking and yielding of reinforcement.

Frequency response spectra at the rear wall were reasonably well predicted by all the three models. Acceleration response spectra results obtained with the IHC layer model and with the Abaqus model applying equal assumptions for tensile cracking behaviour were similar. The in-house code is flexible for parametric studies and comparisons with Abaqus. It should be noted that the assumed structural damping affects the response spectra results. Sensitivity studies on damping assumptions are presented in Saarenheimo et al. (2017).

REFERENCES

Abaqus Theory Manual. (2014). Version 6.14-1. Dassault Systèmes.

- Bathe, K.-J. and Dvorkin, E.N., (1985). A four-node plate bending element based on Mindlin/Reissner plate theory and mixed interpolation. *International Journal for Numerical Methods in Engineering*, 21 367-383.
- Calenberg Ingenieure GmbH. bi-Trapez Bearing®. <http://www.calenberg-ingenieure.com/pr-building-construction-da-elastomeric-impact-sound-insulation-bi-trapez-bearing.htm/> (accessed 6.7.2016).
- Chopra, A.K. (1995). *Dynamics of Structures*, fourth ed. Prentice Hall. London.
- Ibrahimbegovic, A. and Frey F. (1993). “Stress resultant finite element analysis of reinforced concrete plates”, *Engineering Computations*, 10 15-30.
- Koehlin, P. and Potapov, S. (2007). “Global Constitutive Model for Reinforced Concrete Plates”. *Journal of Engineering Mechanics*, 133 257-266.
- Riera, J.D. (1968). “On the stress analysis of structures subjected to aircraft impact forces”. *Nuclear Engineering and Design*, 8, 415–426.
- Saarenheimo, A., Calonius, K., Fedoroff, A., Tuomala, M. and Vepsä, A. (2017) ” Numerical sensitivity studies on vibration propagation and damping”. *Transactions, SMiRT-24*, Busan, Korea, Division V.
- Vepsä, A., Aatola, S., Calonius, K. and Halonen, M. (2015). “Impact testing of a wall-floor-wall reinforced concrete structure”. *Transactions, SMiRT-23 Manchester*, United Kingdom - August 10-14, 2015, Division V, Paper ID 337.